1-2014

A multi-method and multi-scale approach for estimating city-wide anthropogenic heat fluxes

Winston T. L. CHOW
Singapore Management University, winstonchow@smu.edu.sg

Francisco SALAMANCA

Matei GERGESCU

Alex MAHALOV

Jeffrey MILNE

See next page for additional authors

Citation

CHOW, Winston T. L., SALAMANCA, Francisco, GERGESCU, Matei, MAHALOV, Alex, MILNE, Jeffrey, & RUDDELL, Benjamin L..(2014). A multi-method and multi-scale approach for estimating city-wide anthropogenic heat fluxes. *Atmospheric Environment, 99*, 64-76.
Available at: https://ink.library.smu.edu.sg/soss_research/3052

Atmospheric Environment 99 (2014) 64–76

Contents lists available at ScienceDirect

Atmospheric Environment

journal homepage: www.elsevier.com/locate/atmosenv

A multi-method and multi-scale approach for estimating city-wide anthropogenic heat fluxes

Winston T.L. Chow [a, *], Francisco Salamanca [b], Matei Georgescu [c], Alex Mahalov [b], Jeffrey M. Milne [d], Benjamin L. Ruddell [e]

[a] Department of Geography, National University of Singapore, AS2, #03-01, 1 Arts Link, Kent Ridge, Singapore 117570, Singapore
[b] School of Mathematical and Statistical Sciences, Arizona State University, USA
[c] School of Geographical Sciences and Urban Planning, Arizona State University, USA
[d] School of Meteorology, University of Oklahoma, USA
[e] Fulton Schools of Engineering, Arizona State University, USA

HIGHLIGHTS

- Urban anthropogenic heat (Q_F) was estimated over different spatial-temporal scales.
- We utilised a novel multi-method approach (inventory and BEM) to estimate Q_F.
- Our approach shows improved Q_F sensitivity to weather vs. previous methods.
- Strong regional variations in Q_F exist, especially notable over space and time.

ARTICLE INFO

Article history:
Received 30 June 2014
Received in revised form
17 September 2014
Accepted 19 September 2014
Available online 20 September 2014

Keywords:
Anthropogenic heat
Waste heat
Urban climate

ABSTRACT

A multi-method approach estimating summer waste heat emissions from anthropogenic activities (Q_F) was applied for a major subtropical city (Phoenix, AZ). These included detailed, quality-controlled inventories of city-wide population density and traffic counts to estimate waste heat emissions from population and vehicular sources respectively, and also included waste heat simulations derived from urban electrical consumption generated by a coupled building energy – regional climate model (WRF-BEM + BEP). These component Q_F data were subsequently summed and mapped through Geographic Information Systems techniques to enable analysis over local (i.e. census-tract) and regional (i.e. metropolitan area) scales. Through this approach, local mean daily Q_F estimates compared reasonably versus (1.) observed daily surface energy balance residuals from an eddy covariance tower sited within a residential area and (2.) estimates from inventory methods employed in a prior study, with improved sensitivity to temperature and precipitation variations. Regional analysis indicates substantial variations in both mean and maximum daily Q_F, which varied with urban land use type. Average regional daily Q_F was ~13 W m^{-2} for the summer period. Temporal analyses also indicated notable differences using this approach with previous estimates of Q_F in Phoenix over different land uses, with much larger peak fluxes averaging ~50 W m^{-2} occurring in commercial or industrial areas during late summer afternoons. The spatio-temporal analysis of Q_F also suggests that it may influence the form and intensity of the Phoenix urban heat island, specifically through additional early evening heat input, and by modifying the urban boundary layer structure through increased turbulence.

1. Introduction

A significant aspect of the growth of cities is the *urban metabolism* function, which is the sum of all materials and commodities produced and/or utilized in order to sustain a city's inhabitants (Wolman, 1965). The generation of waste heat, water and pollutants

* Corresponding author.
E-mail addresses: winstonchow@nus.edu.sg, wtchow@asu.edu (W.T.L. Chow).

http://dx.doi.org/10.1016/j.atmosenv.2014.09.053

into the atmosphere from the metabolism directly alters near-surface urban climates, especially over different spatial and temporal scales (Oke, 2006). One prominent feature in urban meteorological research is the input of anthropogenic heat and moisture emissions associated with energy consumption from various sources within cities. These can originate through consumption of electricity and heating fuels originating from buildings or industrial activities, combustion of fuel from vehicular traffic, and activities associated with human metabolism; these inputs are hereafter referred to as Q_F (Sailor, 2011).

The influence of Q_F on local-scale urban climates can be considerable. Within mid- or high-latitude cities during winter, waste heat from urban metabolism can be significant in urban heat island (UHI) development (e.g. Magee et al., 1999; Fan and Sailor, 2005). This feature arises due to smaller geographical input of solar radiative fluxes relative to low-latitude cities, as well as comparatively thinner winter urban boundary layers when compared to warmer, more turbulent summer conditions. This impact of Q_F on surface air temperatures may not be restricted to cities and their nearby environs. Given the rapid rate of global urbanization, and corresponding rates of energy consumption, there is a possibility that combined waste heat from multiple large cities could also increase winter nocturnal near-surface temperatures at regional scales e.g. the North American and European continents (Zhang et al., 2013).

Q_F is a component of the urban Surface Energy Balance (SEB), and SEB is quantified by the following equation of flux densities (Oke, 1988):

$$Q^* + Q_F = Q_H + Q_E \pm \Delta Q_S \pm \Delta Q_A \left(\mathrm{Wm^{-2}}\right) \quad (1)$$

where Q^* = net all-wave radiation, Q_H = sensible heat, Q_E = latent heat, ΔQ_S = net heat storage, and ΔQ_A = turbulent heat advection into the urban system.

Existing urban SEB work is primarily focused on observation, e.g. through eddy covariance (EC), or modeling e.g. through numerical or physics-based models of other terms in Equation (1) apart from Q_F (e.g. Grimmond et al., 2010). In contrast, there are three extant approaches to directly estimating Q_F. First, by the inventory of electrical consumption across different urban sectors, such as from buildings, industry and transport. Second, via Q_F based on accurate parameterizations of coupled building energy models that simulate waste heat rejected into the atmosphere of regional or global climate models. Third, through derivation of waste heat from closure of urban SEB using EC flux data residuals. Sailor (2011) reviewed several methodological limitations with respect to each of these methods, such as the lack of data availability over differing spatio-temporal resolutions for the inventory of Q_F arising from buildings, industry and transport; the relative complexity and computational cost of running coupled building energy-regional climate models; and the high cost of installing and logistical difficulties in operating an urban EC tower for estimating the urban SEB, as well as its implicit error uncertainties with respect to EC data residual accuracy. Notably, he suggested that future research should consider utilizing a combination of these approaches in estimating Q_F.

Despite these limitations, research originating from several European (e.g. Christen and Vogt, 2004; Offerle et al., 2005; Pigeon et al., 2007; Allen et al., 2010; Iamarino et al., 2012; Bohnenstengel et al., 2013; Lindberg et al., 2013; Ward et al., 2013), Asian (e.g. Ichinose et al., 1999; Dhakal and Hanaki, 2002; Lee et al., 2009; Quah and Roth, 2012), Australian (Simmonds and Keays, 1997), and North American cities (e.g. Taha, 1997; Sailor and Lu, 2004; Fan and Sailor, 2005; Grossman-Clarke et al., 2005; Salamanca et al., 2013, 2014) enable us to infer several observations about Q_F:

- Spatial variations in urban land-use are important in Q_F with largest mean fluxes originating from areas with commercial or industrial land-uses, which generally have greater energy demand and consumption compared to residential land-uses. The former land-uses are usually concentrated in urban downtown core areas, while the latter corresponds with suburban areas or the urban-rural boundary. Coincidentally, this spatial pattern of Q_F matches the typical distribution of the UHI intensity across a city (Oke, 1982). Further, areas adjacent to major traffic thoroughfares (e.g. highways/freeways) were also associated with relatively higher Q_F compared to areas with local roads due to greater volume of vehicle heat and moisture emissions.
- Temporal variations are also significant in Q_F dynamics. In sub-diurnal or hourly time scales, peak fluxes tend to coincide with both morning and evening rush hour periods, and can be a large component of the urban energy balance relative to other radiative (i.e. incoming short-wave and outgoing long-wave with respect to the urban surface) or turbulent transfer (i.e. sensible and latent heat) terms. On longer time scales (daily, monthly or annual), this may not be the case. Taha (1997) noted that daily mean Q_F flux in city centers (e.g. 20–40 W m^{-2} in summer) are much smaller compared to mean incident shortwave radiation, which is usually an order of magnitude larger.
- The seasonal impact of Q_F largely depends on a city's geographical location. On average, Q_F fluxes are greater during winter in mid/high-latitude cities, where waste heat from residential heating is greater than those generated from summer air-conditioning in low-latitude cities. For most cities, more energy is consumed through heating, rather than cooling, to maintain a comfortable ambient temperature for human thermoregulation (Hill et al., 2013). For instance, Ichinose et al. (1999) noted in their model simulations in Tokyo (35.6 °N) that a remarkable peak winter hourly Q_F of ~1590 W m^{-2} occurred in the downtown/commercial area of the city, with most of this waste heat originating from building hot water supplies for indoor heating. In contrast, Quah and Roth (2012) estimated that a maximum hourly Q_F in downtown Singapore (1.4 °N), where building interior cooling via air conditioning is prevalent, was ~113 W m^{-2}.

In the majority of previous research, Q_F estimates were restricted to a single method (i.e. assessing waste heat through inventory, energy balance residual from an EC tower, or through extant building energy models). Although Offerle et al. (2005) and Pigeon et al. (2007) were notable exceptions as they used multiple methods in estimating Q_F for Lodz and Marseille respectively, their analyses were restricted to a single, local spatial scale (<1 km^2). There remains a gap in the extant literature for the application of multiple-method approaches for Q_F analysis as suggested by Sailor (2011). A useful application of this combined approach would enable examination of Q_F across multiple spatial and temporal resolutions, which potentially yields useful results in interpreting these Q_F data. Thus, in this study, we use a variety of methods to map and analyze Q_F for a major city – Metropolitan Phoenix, Arizona – at both local (i.e. for a residential neighborhood around an EC tower) and meso-scales (i.e. for the entire metropolitan area). We attempt to answer the following research questions: (1.) what are the typical summer Q_F profiles across metropolitan Phoenix; (2.) what are the relative contributions of building energy consumption, emissions from vehicular traffic, and human metabolism towards these distributions of Q_F, and; (3.) how do these profiles compare with derived local-scale EC flux residuals from a residential area?

2. Study area

The Metropolitan Phoenix area (33.4 °N, 112.0 °W; hereafter referred to as Phoenix unless specified otherwise) is among the most extensive urban agglomerations in the United States, with a current size of ~37 000 km^2. It has also been subject to rapid growth in population, from 0.73 million in 1960 to 4.2 million in 2010 (U.S. Census, 2010). Much of Phoenix's land cover is residential in land-use, although small concentrations of commercial and industrial land-uses are found in the downtown core of its component towns and cities (Fig. 1). As with several other large urban areas in the Southwest U.S., the primary mode of transportation is through the automobile, which has enabled both its large suburban land cover and the dense network of roads and highways that are laid out in a North-South and East-West grid system (Gober, 2006). The urban area is subject to a hot desert climate (Köppen classification *BWh*), with extremely hot summers where maximum daytime temperatures regularly exceed 43 °C. Thus, greater energy demand in summer for interior cooling of buildings, mostly through the extensive use of air-conditioning systems, is prevalent throughout the metropolitan area.

The city has also been a prominent foci for urban climate research, especially for documenting the physical basis of the UHI through a variety of approaches (e.g. Brazel et al., 2007; Chow et al., 2012; Georgescu et al., 2012, 2013), the influence of exposure from extreme temperatures on its resident population, as well as attempts to mitigate or reduce this exposure (e.g. Harlan et al., 2006; Declet-Barreto et al., 2013; Hondula et al., 2014), and the dynamics of particulate air pollution with respect to boundary layer development (Lee et al., 2003; Fernando et al., 2010). As with other cities, the examination of Q_F has been less rigorous, although Grossman-Clarke et al. (2005) used the inventory method suggested by Sailor and Lu (2004) to estimate mean hourly Q_F fluxes for three distinct land cover classes – urban built-up (*i.e.* the urban core), mesic residential (with yard surfaces dominated by flora requiring intensive summertime irrigation), and xeric residential (with yard surfaces covered by native or desert-adapted vegetation requiring less irrigation). They noted the presence of a dual peak of Q_F corresponding with the morning (0700–0800 h) and evening (1700–1800 h) rush hours. The magnitude of this peak varied with land-use class, with xeric residential (urban built-up) land-use having the largest (smallest) mean emissions of waste heat per unit area throughout the day. The latter result is notable, given that it is contrary to previous studies documenting peak Q_F fluxes occurring at the urban core. They also noted that the influence of Q_F on urban temperatures is greatest in the early evening when waste heat emissions are largest, and corresponding with the development of larger UHI intensities.

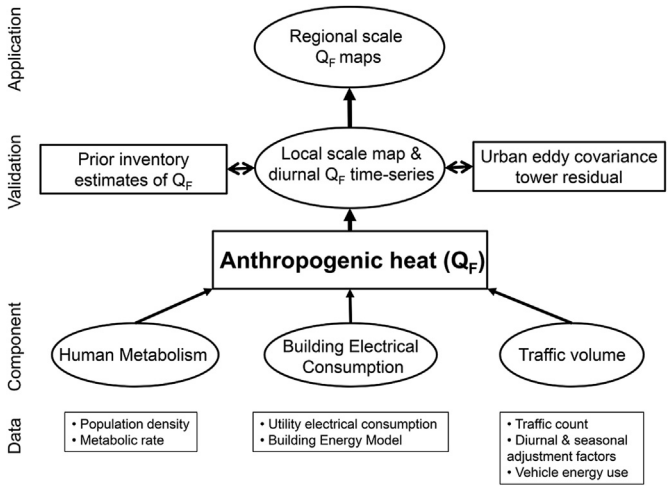

Fig. 2. The multi-method approach utilized in this study to estimate Q_F across multiple spatial scales.

3. Methodological framework

A brief schematic of our approach to estimate the anthropogenic heat for Phoenix is presented (Fig. 2). Here, Q_F within the urban canopy layer (i.e. from surface to mean roof height) for a period p and location i was estimated as the sum of three sub-components of urban waste heat in Phoenix, which were composed from human metabolism (M), air conditioning from buildings (B), and traffic volume (T) respectively:

$$Q_{F(i,p)} = Q_{FM(i,p)} + Q_{FB(i,p)} + Q_{FT(i,p)} \left(\mathrm{Wm^{-2}}\right) \quad (2)$$

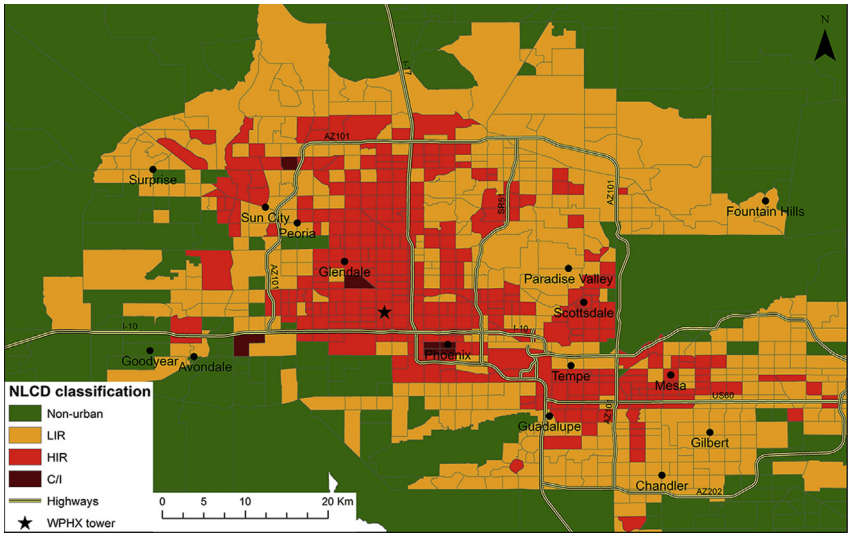

Fig. 1. The Phoenix metropolitan area and associated land cover as per Fry et al. (2011) mapped over 2010 U.S. Census tracts. LIR = Low-intensity residential; HIR = High-intensity residential; C/I = Commercial or Industrial land use. The location of the EC tower (WPHX) used for comparisons with Q_F data is marked on the map.

We applied different methods and datasets to obtain each Q_F sub-component. The impact of human metabolism and traffic volumes in Phoenix were estimated through existing, publicly available databases via top-down inventory methods (e.g. Grimmond, 1992; Sailor and Lu, 2004), while the waste heat directly rejected from building electrical use through air conditioning was derived through the application of the Building Energy Model (BEM) (Salamanca et al., 2010, 2013, 2014). These component data are subsequently summed as per equation (2) for different spatio-temporal scales i.e. local-scale, neighborhood Q_F time series, as well as regional-scale maps of Q_F distributed across Phoenix. Local-scale Q_F data obtained by our multi-method approach are also compared against Q_F data through SEB residual data from urban EC flux tower, and prior inventory Q_F estimates from estimated by Grossman-Clarke et al. (2005) [hereafter GC05] for similar land cover categories.

Regional-scale Q_F are mapped using ArcGIS (version 10.1, ESRI systems) for the metropolitan area. Both Q_{FT} derived at each traffic count station, and Q_{FB} from BEM, were geo-referenced as point/raster data according to the latitude and longitude from traffic counting locations and 1 km model grid centroids respectively. Q_{FM} data, however, were plotted as vector data based on demographic information obtained from tract areas based on the U.S. Census (2010) designations (Fig. 3). As these tracts are the coarsest spatial resolution available to enable analysis of total Q_F through equation (2), the former raster data were subsequently summarily averaged, aggregated and spatially joined to each census tract within the study area through ArcGIS; thus, these census tracts were the scale of measurement used for regional-scale multi-method Q_F analysis.

We applied this framework for data analysis during a 78-day period within the summer of 2012 (June 15–August 30). We selected this period based upon the large energy demand for building air-conditioning during summer, which historical electrical utility data show as the peak period of annual electrical consumption. Notably, emissions from heating fuels such as fuel oil and natural gas typically used in winter within buildings in cold climates were assumed to be negligible in this season, and can be excluded from this analysis. As Sailor (2011) noted, inventory methods to estimate Q_F are complicated by the relatively coarse temporal resolution of its databases. Thus, wherever possible, we also attempt to refine these data by accounting for temporal variance (e.g. implementing scaling factors for weekday vs. weekend and seasonal influences on traffic and population data), which would affect accuracy of Q_F estimates.

3.1. Q_F emissions from human metabolism

Human biological activity produces metabolic heat that varies with the activity type, time of day, and the population density within the area of interest. In general, metabolic rates (*MR*) from typical daytime activity types (e.g. driving, walking, domestic and office work) can be 2 to 3 times greater in magnitude vs. passive activities associated with nighttime (e.g. sitting, sleeping). Fanger (1972) lists estimates of energy produced from human metabolism, and in our study, we used typical mean *MR* values of 180 W during daytime, and 70 W at night. These magnitudes are similar to previous estimates of Q_{FM} (Sailor and Lu, 2004; Pigeon et al., 2007; Quah and Roth, 2012). We have also distinguished between daytime (0700–2100 h) and nighttime (2200–0600 h) hours during the summer season, with an hourly transitional period in between where *MR* is linearly interpolated between daytime and nighttime magnitudes.

Our approach also used 2010 U.S. Census data to derive specific waste heat contributions from census tracts ($n = 916$) for the two counties comprising Phoenix's boundaries: Maricopa and Pinal. Total population data from each tract were divided by its respective area to obtain a population density. Subsequently, we examined census tracts associated with downtown areas in Phoenix (i.e. the city's urban core) ($n = 7$) to account for diurnal changes in daytime resident population during weekdays. Previous U.S. census data have shown that a significant decrease in population occurs in

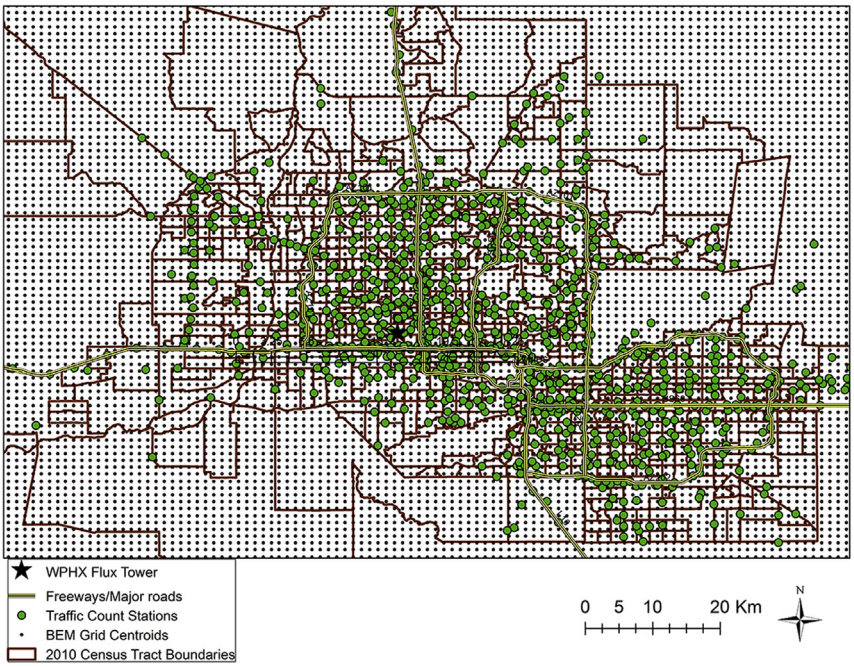

Fig. 3. Location of (1.) traffic count locations for deriving Q_{FT}, (2.) census tract boundaries as specified by the 2010 U.S. Census for Q_{FM}, and (3.) 1 km grid centroids from BEM in which Q_{FB} was modeled.

residential areas due to weekday work commutes within numerous US cities, and we subsequently applied a commute factor of −7.3% (+7.3%) towards population density from 0800 to 1700 h during weekdays for identified residential (downtown core) areas to account for the dynamic shift in workday population in Phoenix (U.S. Census Bureau, 2000). Thus, we based our estimates of Q_{FM} for a given period via calculating the approximate hourly population density within a given Phoenix census tract (ρ_{pop}), and the typical human *MR* in the following equation:

$$Q_{FBM(i,p)} = \rho_{\text{pop}(i,p)} \times MR_p \left(\text{Wm}^{-2}\right) \quad (3)$$

3.2. Q_F emissions from building electrical consumption

BEM is a building energy model integrated in the multilayer urban canopy parameterization (BEP, Martilli et al., 2002) that takes into account the exchange of energy between the buildings and the overlying atmosphere as well as the impact of the air conditioning (AC) systems (Salamanca et al., 2010; Salamanca and Martilli, 2010). BEP + BEM was officially coupled in the non-hydrostatic (V3.2) version of the Weather Research and Forecasting WRF (Skamarock et al., 2008) model.

In BEM, a building in an urban block is treated as a pile of boxes, each box representing a particular building floor. The time evolutions of the indoor air temperature and moisture are computed explicitly for each floor solving an energy conservation equation that takes into account the heat generated by the equipment and occupants within buildings, radiation through windows, natural ventilation, heat diffusion through walls and roofs, and the AC systems. This time evolution is accounted for via a step function representing typical building activity during a 24 h period. While there is a possibility that waste heat from building occupants may be double-counted with the inventory method detailed in Section 3.1 during the daytime, the step function utilized likely overestimates this metabolism component at night when minimal biological activity occurs. When the indoor temperature reaches a fixed target, all the "extra" sensible heat (Q_H) is extracted by the AC systems to maintain a constant indoor temperature. The total electric consumption (ELC) is then computed and the sensible heat Q_{FB} (ELC + Q_H) is released into the atmosphere as a source of Q_F.

Salamanca et al. (2013) simulated urban AC energy consumption for several extreme heat events over the semiarid metropolitan area of Phoenix with the WRF model coupled to the multilayer building energy parameterization BEP + BEM. WRF-simulated AC consumption compared favorably to observationally derived AC consumption supplied by an electric utility company in terms of both amplitude and timing. For the results presented here, we considered the same set-up described in the former work. We used the non-hydrostatic (V3.4.1) version of the WRF model to evaluate Phoenix waste heat release due to AC. WRF simulations were conducted with the initial and boundary conditions obtained from NCEP FNL data (number ds083.2) with a spatial resolution of $1^\circ \times 1^\circ$ and a temporal resolution of 6 h. The horizontal domain was composed of four two-way nested domains and included 40 vertical levels.

The inner domain had a grid spacing of 1 km and covered the complete Phoenix metropolitan area. The US Geological Survey (USGS) 30 m 2006 NLCD06 (Fry et al., 2011) was used to represent modern-day land use-land cover (LULC) for the urban domain. Three different urban classes were defined to describe the morphology of the city: commercial or industrial (C/I) areas which are associated with business, manufacturing and trade land use; high-intensity residential (HIR), related to higher-density and older, more established residences in Phoenix; and low-intensity residential (LIR) in which lower population densities and more recently developed housing communities are found. Further information about average and standard deviations of typical building morphological characteristics associated with these categories can be found in Burian et al. (2002).

Two important assumptions are noted regarding LULC classification. First, while we have grouped commercial and industrial areas within a common urban class for modeling Q_{FB} based on building morphological characteristics, we are cognizant that industrial facilities may have significantly larger on-site electrical and fuel consumption and generation of waste heat that will not be accounted for in BEP + BEM. Given the difficulties in obtaining detailed energy data from these infrequent point sources in Phoenix, coupled with the lack of current modeling approaches that can resolve these heat emissions at local scales, we believe that the omission of measures to account for these processes is acceptable in the context of this study. Second, we also assumed that all waste heat to the urban canopy layer is partitioned as Q_H. While we acknowledge that some cooling energy could be emitted as Q_E, which could be a significant SEB input at the local spatial scale especially from large cooling towers, the presence of these towers is largely limited to C/I areas in Phoenix which comprise <1% of extant land cover for our study area. In addition, no such towers are located near an EC flux tower used in this study for local-scale Q_F comparisons.

We subsequently conducted five independent 15-day simulations covering the complete summer-period from June 15 to August 30 2012. Each simulation started 7-h previously, and this time-interval was considered as the model spin-up period. Results of Q_{FB} from these BEM simulations were subsequently geo-referenced as point/raster data based on the latitude and longitude of the 1 km model grid centroid, and spatially joined to the vector Q_{FB} data at the census-tract scale.

3.3. Q_F emissions from vehicular traffic

There are three methodological steps applied towards calculating Q_{FT}. First, traffic estimates were obtained from several sources that conducted traffic counts throughout the metropolitan Phoenix area. These include recent public databases compiled by the City of Phoenix (2010), Maricopa County (2012), and the Arizona Department of Transportation (2010), in which we compiled data from 1052 traffic count stations scattered throughout the study area (Fig. 3). These stations covered a range of road types from highways, arterial, collector and local roads. For the purposes of urban transportation management and planning, the aforementioned agencies convert the raw counts of vehicular traffic from counting stations into a quality-controlled Average Annual Daily Traffic (AADT) volume over a given road section. Temporal variations are subsequently accounted for through applying an hourly fractional traffic profile based on typical distribution of traffic volume during the day, and the seasonal profile of mean traffic count variation over the course of a calendar year. These profiles are based on data collected by the Maricopa Association of Governments (MAG) (2011), and are subsequently applied for all AADT data compiled in this study.

Notably, the sizeable morning and evening peaks of increased vehicular traffic occurring during rush hours, with a larger peak during the evening period, are similar to diurnal traffic data patterns reported from other major U.S. cities (e.g. Hallenbeck et al., 1997; Kim et al., 2008). The monthly data illustrate that traffic volumes in Phoenix are substantially higher during the winter and spring seasons vs. the summer. This is primarily due to the city hosting numerous out-of-state visitors during the former period

due to more favorable weather compared to other parts of the country. This contrasts with the national average for vehicle travel in the U.S., in which more car use occurs in the summer vs. winter (U.S. Federal Highway Administration, 2013).

The second step is to compute the mean energy released per vehicle per meter (*EV*). We utilized the following approach used by Sailor and Lu (2004):

$$EV = NHC \cdot \rho_{\text{fuel}} \Big/ FE \left(\text{Jm}^{-1}\right) \quad [4]$$

where *NHC* = mean net heat of vehicular gasoline and diesel combustion (J kg^{-1}), which is estimated to be ~4.46 × 10^6 J kg^{-1}; ρ_{fuel} is the mean density of gasoline and diesel (kg l^{-1}), which is ~0.7664 kg l^{-1}, and *FE* is the mean vehicle fuel economy (km l^{-1}).

Based on monthly on-road gasoline vs. diesel consumption data from the Arizona Department of Transportation (2010), we can discern that there is an approximate 4:1 split between gasoline and diesel use respectively in the state, and we assume a similar breakdown for traffic in Phoenix. Given this proportion, and by using published estimates of NHC and ρ for gasoline (4.5 × 10^6 J kg^{-1}; 0.75 kg l^{-1}) and diesel (4.3 × 10^6 J kg^{-1}; 0.832 kg l^{-1}) (U.S. Energy Information Administration, 2014), combined with mean *FE* data for all motor vehicles in the U.S. is 7.5 km l^{-1} (or 17.6 miles per gallon) in 2010 (U.S. Department of Transportation, (2011)), we estimated mean *EV* is 4558 J m^{-1}, which falls between the mean *EV* of 3975 J m^{-1} reported in Sailor and Lu (2004) for several U.S. cities, and 4710 J m^{-1} estimated by Pigeon et al. (2007) for Marseille. An important caveat is that a small proportion of energy of fuel combustion is converted to and evaporated as water vapor, and a conservative estimate of this is ~8% of total vehicular emissions (as per Pigeon et al., 2007). This latent heat partitioning could affect comparisons with local-scale Q_F – especially in arid climates where substantial changes in Bowen ratio could occur even with minor variations in Q_E input into the local urban energy balance – and should be noted accordingly.

The final step was to combine these *EV* and traffic count data to derive a mean Q_{FT} that is representative around each traffic count station. This was based on the approach adopted by Grimmond (1992) in the city of Vancouver:

$$Q_{FT(i,p)} = \left(TC_{(i,p)} \cdot RL \cdot EV / A \cdot t\right) \left(\text{Wm}^{-2}\right) \quad [5]$$

where *TC* = normalized traffic count at location *i* during period *p*, *RL* = mean road length (km); *A* = source area of traffic (km^2), and *t* = time (taken to be 1 h or 3600 s). In this study, *RL* for each location *i* was calculated by the point-to-point distance between each traffic count station and its closest adjacent neighbor. At the city boundary, the sparse number of stations would considerably increase *RL*; to ensure consistency in our Q_{FT} comparisons, maximum *RL* is capped at 1.6 km (or 1 mile). This distance was selected as it was the median distance between traffic count stations in the compiled database. *A*, which represents the average area in which traffic conditions are representative of the traffic count location, was conservatively assumed to be 1 km^2 for the urban area.

3.4. Estimates of local-scale Q_F from eddy flux tower

Several components of the local-scale surface energy balance were directly measured at an EC tower sited in West Phoenix (WPHX: 33.4838 °N, 112.1426 °W). The tower is sited in a suburban residential neighborhood (HIR as per Fry et al., 2011) mostly comprising of low-rise, single-story housing with minimal vegetated surface cover, with most of its source area for both

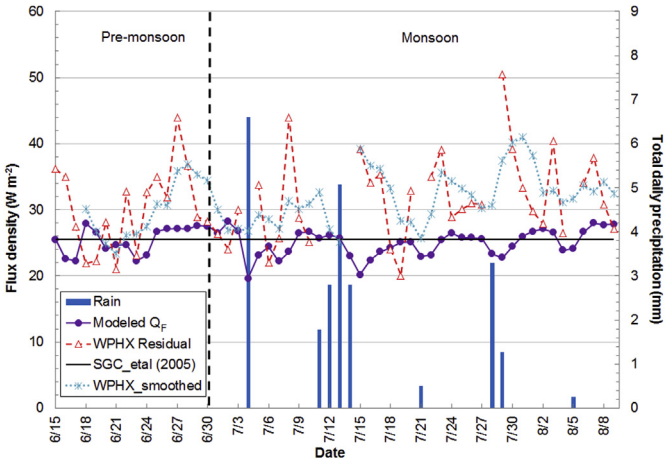

Fig. 4. Mean time series of daily Q_F at WPHX taken from the multi-method model compared with WPHX mean residuals ($\overline{R}$) and a mean daily Q_F from the inventory method of GC05 for a xeric residential land cover category. Precipitation events during the study period at WPHX are noted as vertical bars.

radiative and turbulent fluxes falling within this land use. Specific details regarding the instrumental setup, measurement heights, projected radiative and turbulent source areas, as well as details on data processing methods can be found in Chow et al. (2014). In this study, the mean daily residual of the tower (*R*) was measured through modifying equation (1) after Pigeon et al. (2007):

$$R = Q^* - (Q_H + Q_E) = \pm\Delta Q_S \pm \Delta Q_A - Q_F \left(\text{Wm}^{-2}\right) \quad [6]$$

The ΔQ_A term is highly sensitive to strong temperature and moisture gradients adjacent to the measurement site, which is generally indicated by discordant changes in urban land-use and/or land cover. Given the tower fetch is ~11 km over mostly homogeneous land use and land cover (Chow et al., 2014), we assume that changes in ΔQ_A during measurements are largely negligible. Variations in *R*, especially during analysis at of temporal periods less than, or in multiples of 24 h, are complicated by this term being the accumulator of systematic measurement errors of the open-path EC process (Oke, 1988). These errors, which include underestimations of observed fluxes, and scale disparities in measurements between radiation and turbulent fluxes, are well known in the EC research literature, e.g. 5–20% for Q^*, Q_H and Q_E (Foken, 2008). The presence of measurement errors, especially arising from periods of low turbulent fluxes, also implies that magnitudes of *R* would generally overestimate "true" values of Q_F.

Further, for sub-24 h time scales, the ΔQ_S term may be the largest term in the urban surface energy balance, especially in hot arid subtropical cities (e.g. Oke et al., 1992). While there are recent attempts to accurately quantify ΔQ_S at hourly scales through a combination of urban canopy modeling and detailed micro-scale measurements with heat flux plates (Aubinet et al., 2012), these methods are not applied here due to lack of specific instrumentation at WPHX required for this purpose. Instead, a daily mean *R* term ($\overline{R}$) is used, in which we assume that daily ΔQ_S ($\overline{\Delta Q_S}$) approximates to zero over 24 h (or 48, 72, 96 h etc.) periods as unrealistic increases in stored heat (and temperatures) of the urban fabric would ensue. Thus, to estimate mean daily magnitudes of Q_F from the flux tower data, we omit the ΔQ_A and ΔQ_S terms over time scales greater than 24 h and are left with:

$$\overline{Q_F} \approx -\overline{R}\left(\mathrm{Wm^{-2}}\right) \quad [7]$$

4. Results and discussion

4.1. Comparison of local-scale Q_F from WPHX tower site

We obtained a 56-day summer period of post-processed EC flux tower data (Jun 15–Aug 13 2012). During days in which no measureable precipitation was measured ($n = 48$), mostly ideal weather conditions (i.e. clear and calm) were present at WPHX. This period also bridged the pre-monsoon (June) and North American monsoon (July and August) months in Phoenix during that year. Using the method outlined in Section 3.4, we obtained $\overline{R}$ for both mean 24 h, and a smoothed 96 h (i.e. 4-day) moving average for non-rain days. These data were compared with the multi-method Q_F obtained from cumulative traffic, BEM and population density data for the census tract in which the WPHX tower was sited in (Fig. 4). Lastly, a daily mean summer Q_F obtained in GC05 for the xeric residential land use category, in which WPHX is located on, was also plotted as a single value over the entire period for comparison.

The mean daily Q_F from the tower $\overline{R}$ (31.3 W m^{-2}), the multi-method approach (25.4 W m^{-2}), and from GC05 (25.6 W m^{-2}) were similar in magnitude for the study's duration. The small disparity in mean 24 h magnitudes of Q_F, reflected in insignificant differences through two-way ANOVA of each method mean ($p > 0.41$), suggests that the three methods applied are potentially viable in estimating waste heat for this location. Unlike the GC05 inventory approach, notable day-to-day variations in Q_F can be observed from both $\overline{R}$ and the multi-method approaches, with the greatest range arising from the 24 h $\overline{R}$ especially after days with rain events. There also appears to be a marked decrease in estimated multi-method Q_F of 2–5 W m^{-2} in the 24 h period immediately after days with observed precipitation. The effect of rainstorms on daily Q_F appears not to persist, however, as diurnal variability of $\overline{R}$ is substantially minimized with the smoothed 4-day plot, as with a corresponding increase in multi-method modeled Q_F in subsequent rain-free days. While these fluctuations in daily $\overline{R}$ could be due to SEB measurement errors (e.g. arising from possible heat energy transfer due to storm runoff drainage away from WPHX), another factor could be due to the cooler temperatures resulting in a more comfortable thermal environment and lower residential AC usage, which is reflected in the reduced mean Q_{FB} estimated during days in which rain events occurred during the monsoon season (Fig. 5). Indeed, much of the variability in this multi-method approach stems from changes in daily Q_{FB} arising through corresponding alterations in average electrical consumption for this location, with both daily Q_{FT} and Q_{FM} being relatively insensitive at the diurnal time scale.

An OLS regression plot of multi-approach modeled Q_F vs. $\overline{R}$, together with the corresponding residual plot (i.e. residual vs. fitted values) and histogram, are also included for analysis (Fig. 6; Table 1). The low correlation between estimates of modeled and $\overline{R}$ is unsurprising given the various implicit assumptions in the latter, although model residuals in the scatterplot (Fig. 6b) are both normal and homogenous. In this analysis, we note that simple correlation measures often do not illustrate model accuracy, which instead can be ascertained by difference measures that include bias, average and mean squared errors shown in Table 1 (Willmott, 1982). In the main, the model underestimates daily Q_F, and has a strong systematic root mean square error (RMSE) that suggests underlying data issues with both the quality of observed data (e.g. implicit errors in estimating $\overline{R}$), as well as in model formulation (e.g. possible unaccounted Q_F input for the WPHX area). However, a reasonable index of agreement ($d = 0.42$) exists despite the low correlation and relatively large error terms. This suggests that the multi-method approach is still useful in predicting Q_F at WPHX, at least for the 24 h time scale. Further development of this approach, or improved methods of estimating

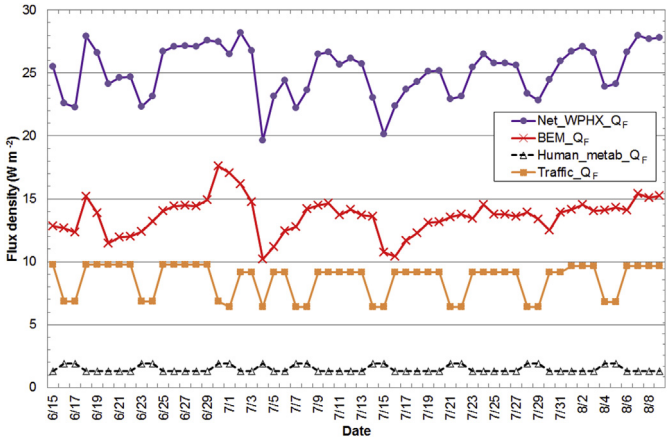

Fig. 5. Mean daily total (Q_F) and sub-component (i.e. Q_{FT}, Q_{FB} and Q_{FM}) time-series plots of waste heat at the WPHX site from the multi-method approach.

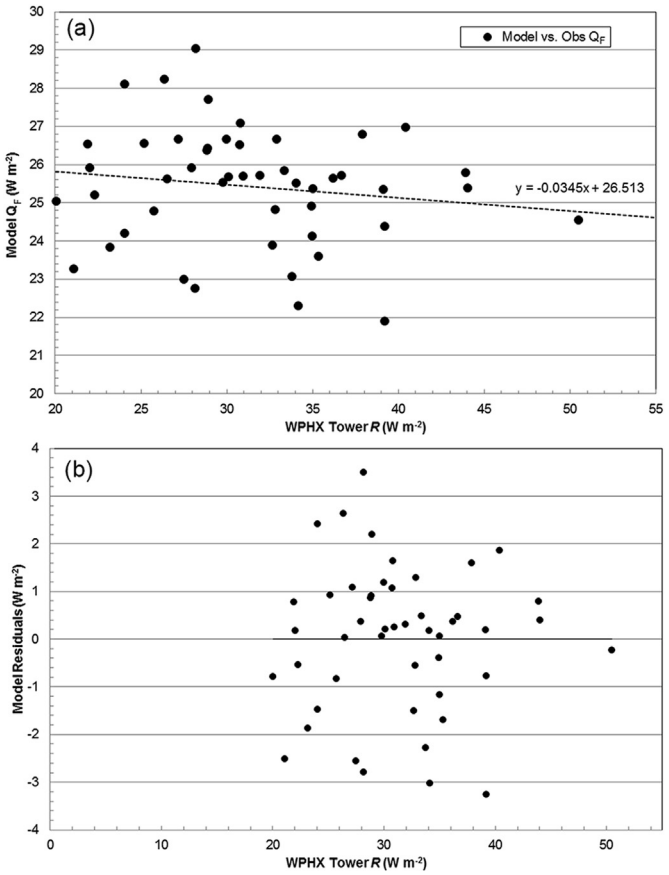

Fig. 6. OLS regression plot of (a.) multi-method modeled daily Q_F vs. observed derived 24 h tower residuals R for WPHX, and (b.) scatterplot of distributed residuals arising from the OLS regression in (a.). Note the normal and heterogeneous distribution of residuals in (b).

Table 1
Quantitative difference measures for multi-method model daily Q_F vs. 24 hr tower R at WPHX.

Difference measure	Magnitude (Wm^{-2} unless indicated)
Mean Absolute Error (*MAE*)	7.04
Mean Bias Error (*MBE*)	−5.89
Root Mean Square Error (*RMSE*)	9.03
Root Mean Square Error − Systematic ($RMSE_S$)	8.91
Root Mean Square Error − Unsystematic ($RMSE_U$)	1.51
Index of agreement (*d*)	0.42 (unitless)

Q_F from$\overline{R}$, may lead to a better estimation of modeled waste heat in subsequent analysis.

Previous research in mainly temperate cities into relationships between mean temperature and estimated Q_F show a strong negative correlation, with larger Q_F present especially during colder winters from residential heating (Offerle et al., 2005; Pigeon et al., 2007; Ward et al., 2013). It is expected the converse should hold for warm (sub)tropical cities where direct emissions into the atmosphere from increased AC is a major contributor towards Q_F variations. A comparison of mean modeled Q_F vs. mean daily temperatures measured at the top of the WPHX tower during both pre-monsoon and monsoon seasons shows a distinct positive relationship between both covariates (Fig. 7), with a stronger correlation ($R^2 = 0.4$) during the monsoon season in which there was a greater range of daily temperatures. While the stronger relationship could be due to higher temperatures observed during the monsoon at WPHX, the increased discomfort due to simultaneous higher ambient humidity conditions may also be a factor that results in greater electrical consumption, intensified residential AC use and larger Q_F.

Although analysis of accurate sub-24 h Q_F from the WPHX $\overline{R}$ was not possible due to methodological limitations, we were able to employ the multi-method approach to derive mean hourly summer Q_F at this location. We compared these hourly profiles of summed total Q_F (as well as hourly component Q_{FM}, Q_{FB}, and Q_{FT}) with hourly Q_F profiles within the urban xeric residential land cover class in Fig. 2 from GC05 (Fig. 8). While peak mean summer Q_F from both methods are similar in magnitude (~35 W m^{-2}) and in timing (early evening coinciding with the rush hour urban commute), two substantial differences between the previous and current estimates of hourly Q_F in WPHX can be seen. First, current estimates of Q_F are consistently ~5 W m^{-2} higher throughout most of the summer; this is best seen during the night from 2000 to 0400 h LT. Second, the morning peak in the previous estimate is absent with the multi-method approach, as a significantly lower Q_F is estimated (30 vs. 15 W m^{-2}). Examination of the components of Q_F at sub-daily time scales suggests that the previous method used in GC05 may have overestimated traffic emissions for this particular residential area, which were previously attributed for the morning rush-hour peak (Sailor and Lu, 2004). The GC05 method may have also underestimated waste heat from residential air-conditioning, especially for the duration of the summer nocturnal period. These differences thus highlight the increased sensitivity of the multi-method approach used in this study towards estimating emissions of Q_F, especially between its components.

4.2. Regional plots of summer Q_F in Phoenix

To examine the spatial variations of waste heat for the regional Phoenix area, we subsequently generated maps of (1.) mean daily

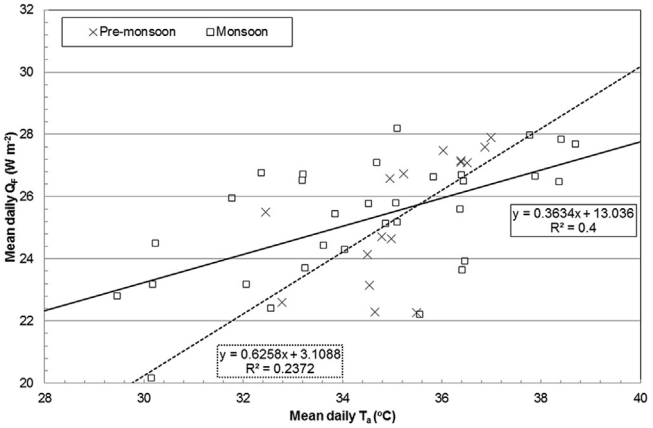

Fig. 7. Correlations between mean daily Q_F and WPHX air temperatures during the pre-monsoon (×, dashed-line OLS regression) and Monsoonal seasons (square, solid line OLS regression). Both correlations are significant at $p < 0.05$.

Q_F and (2.) maximum daily Q_F (i.e. at 1700 h LT) for the summer months in which data were available for each designated census tract in Phoenix (Figs. 9 and 10). The mean and maximum daily Q_F reported for each LULC class, as well as a regional average for the entire study area are also reported (Table 2). While the average daily summer Q_F for metropolitan Phoenix is ~12.8 W m^{-2}, distinct spatial variations according to land cover class are apparent. Notably, higher magnitudes of average Q_F were not found along areas characterized as commercial or industrial areas, but are instead located in older, HIR areas in Phoenix where highest population densities are sampled (Fig. 1; Table 2). In contrast, lower average Q_F are discerned at the LIR areas sited along the margins of the metropolitan area, in which more rapid urbanization − in terms of land conversion from agricultural or desert areas towards residential land uses − has been detected in recent years (e.g. Brazel et al., 2007). While the spatial patterns of mean and maximum daily Q_F are similar, a key difference is that maximum daily Q_F appears to be strongly influenced by waste heat arising from local traffic emissions (Fig. 10). During the evening, consistently larger Q_F is observed in areas that are near to major traffic routes. This is unsurprising given the peak volumes of observed traffic counts and Q_{FT} occurring during the evening rush hour along these commute routes. Lastly, a small but discernable reduction in mean and

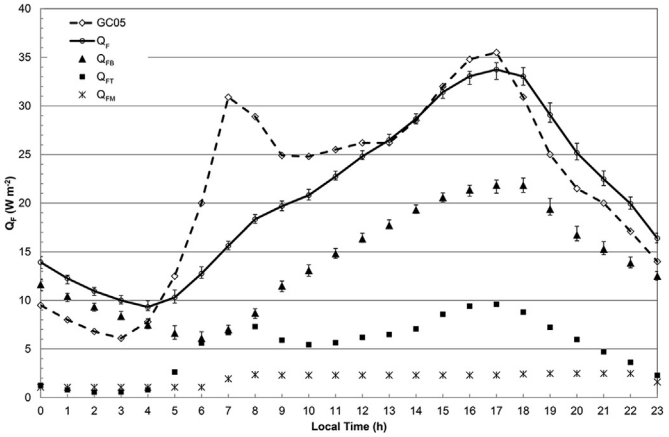

Fig. 8. Hourly profiles of Q_F at WPHX from the inventory method used in GC05, vs. the multi-method approach of estimating Q_F this study. Note that the Q_F subcomponents are plotted as points. Error bars indicate maximum and minimum values of during the sampling period at WPHX.

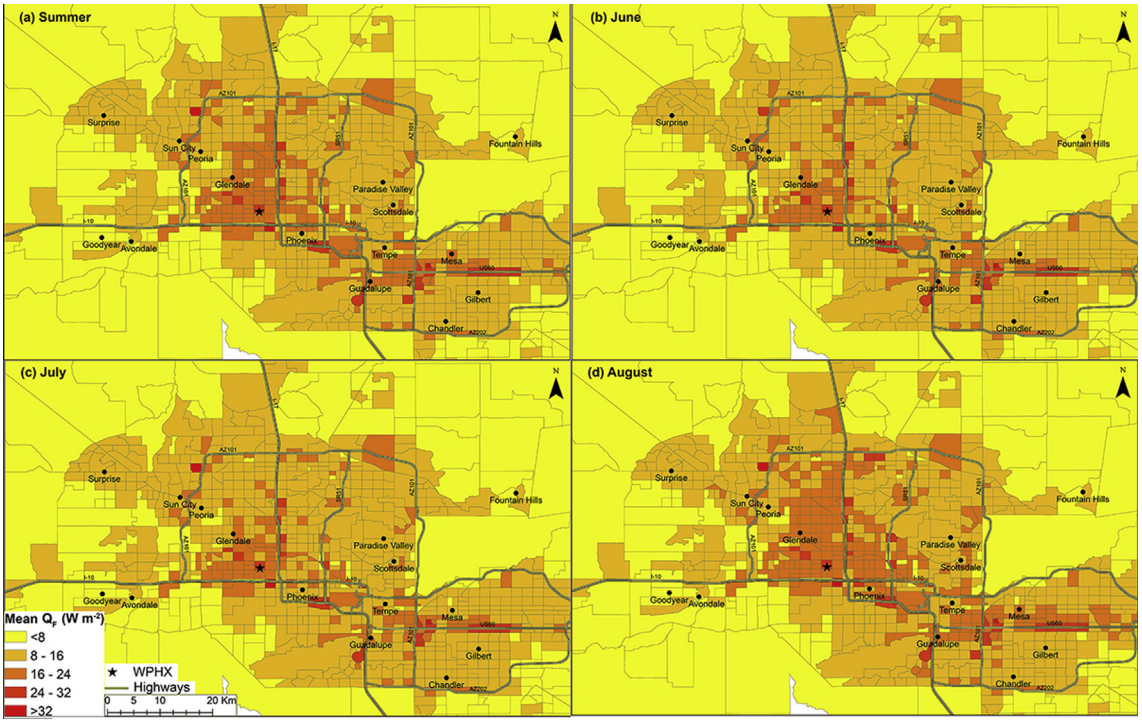

Fig. 9. Mean regional daily Q_F for the Phoenix area during (a.) summer, (b.) June, (c.) July, and (d.) August 2012.

Fig. 10. Same as Fig. 9, but for mean daily maximum Q_F observed at 1700 h LT.

maximum daily Q_F can be seen during the month of July, which can be attributed to lower urban electrical consumption and smaller traffic volume in Phoenix during this period.

We also analyzed variations in mean derived hourly Q_F, as well as its traffic, population and BEM components, between each urban land cover class for the entire summer period (Fig. 11), and we also examined the quantitative distribution of each component through boxplots of all summer data (Fig. 12). This enabled comparisons of hourly Q_F between this multi-method approach with previous reported data from GC05. Although we note that while differences exist between land cover classification between the Stefanov et al. (2001) database used in GC05 with the Fry et al. (2011) database

Table 2
Mean and maximum daily summer Q_F reported at different spatial scales within the Phoenix area.

	Daily summer Q_F (W m^{-2})	
	Maximum (at 1700 h LT)	Mean
Local-scale (LULC class & location description)		
HIR (Census Tract 1127) – high density residential area adjacent to two interstate freeways near central Phoenix	62.427	38.144
C/I (Census Tract 6176) – large commercial mall adjacent to major state highway near Peoria	51.623	32.819
LIR (Census Tract 1167.09) – low density residential area adjacent to intersection between interstate and state highway near Guadalupe	48.013	29.322
Meso-scale (regional)		
Metropolitan Phoenix (average of 916 total urban census tracts)	20.514	12.879

used in this study, several similarities in urban form and function between each category pair (i.e. urban built-up = C/I, xeric residential = LIR, and mesic residential = HIR) enables a basic, qualitative comparison between studies.

As with the local-scale analysis at WPHX, the mean summer Q_F between average regional-scale land cover classes reported here significantly differs with previous estimates in GC05 terms of both magnitudes and trends. These include (1.) a much larger peak Q_F occurring during the evening rush hour within the C/I land cover (54 W m^{-2}) than is reported for all of the urban classes in GC05 (i.e. 35 W m^{-2}); (2.) a smaller evening maximum Q_F for both residential categories (between 22 and 25 W m^{-2}) in this study compared to GC05 (between 30 and 35 W m^{-2}), and (3.) the double maxima of Q_F reported in GC05 is not apparent in this study; instead, a much smaller estimated morning peak Q_F for all land cover classes is evident. Possible factors that can explain these differences between studies include a much smaller average contribution of Q_{FT} that can be discerned throughout the study area (but best observed in LIR areas) from more accurate traffic count data, as well as a larger Q_{FB} associated with higher electrical consumption within C/I areas.

Several important aspects of hourly regional-scale summer Q_F can be seen when examining the distribution of each its components across land cover types (Fig. 12). The largest magnitudes of Q_{FT} are observed in both LIR (>45 W m^{-2}) and HIR (>35 W m^{-2}), and the dual-peak pattern in the morning and evening are seen in all three urban classes; however, the strong positive skew of Q_{FT} in both residential classes indicates that much lower traffic counts (especially from non-highway traffic) are the norm within the majority of residential areas in Phoenix. These differences in traffic waste heat within residential areas should be considered in subsequent research, especially when previous inventory methods assume equal distribution of Q_{FT} throughout an urban area. The daily sinusoidal Q_{FB} trend of is apparent for all three urban classes, but the spread, specifically the observed strong negative skew, is more significant in both LIR and HIR. This feature can be associated with lower electrical consumption in areas around the margins of the metropolitan area, where population densities are relatively lower. Lastly, although there are some exceptions from areas with higher population densities, waste heat from human metabolism is a minor contributor towards total Q_F, with average magnitudes of hourly Q_F within all urban classes of <1 W m^{-2}. It could be possible for future studies to discount Q_{FM} altogether, especially if population densities are low in cities with large, spatially spread-out suburban areas (e.g. most of the Southwestern USA) vs. densely-built cities with large concentrations of high-rise residential buildings (e.g. New York City, Tokyo, Singapore).

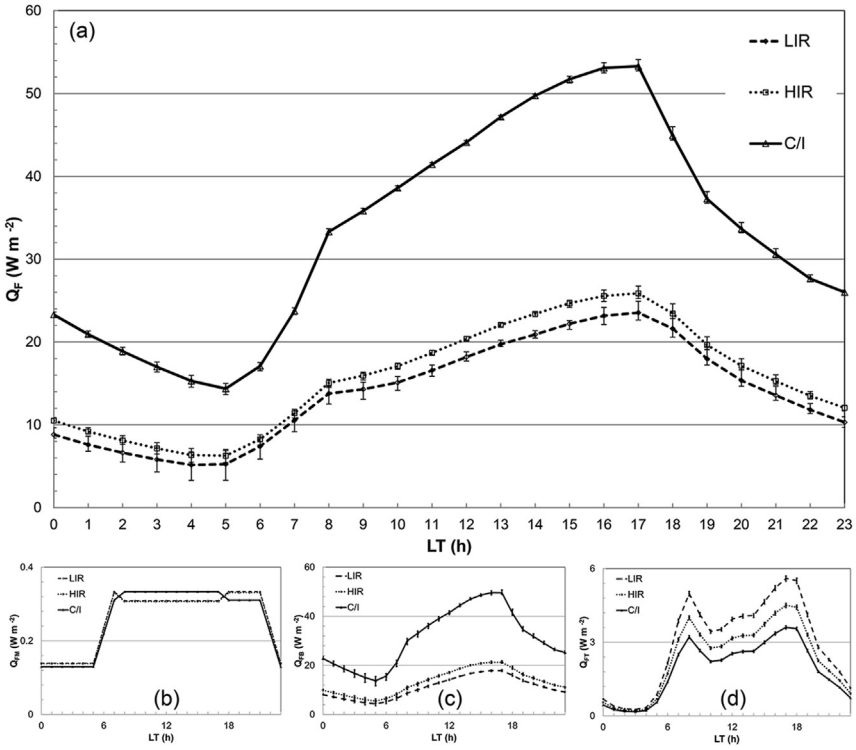

Fig. 11. Mean multi-method hourly summer Q_F for each land cover category listed in Fig. 1 (a.), and each component: (b.) Q_{FM}, (c.) Q_{FB}, and (d.) Q_{FT}. Error bars indicate monthly maximum and minimum flux densities of Q_F.

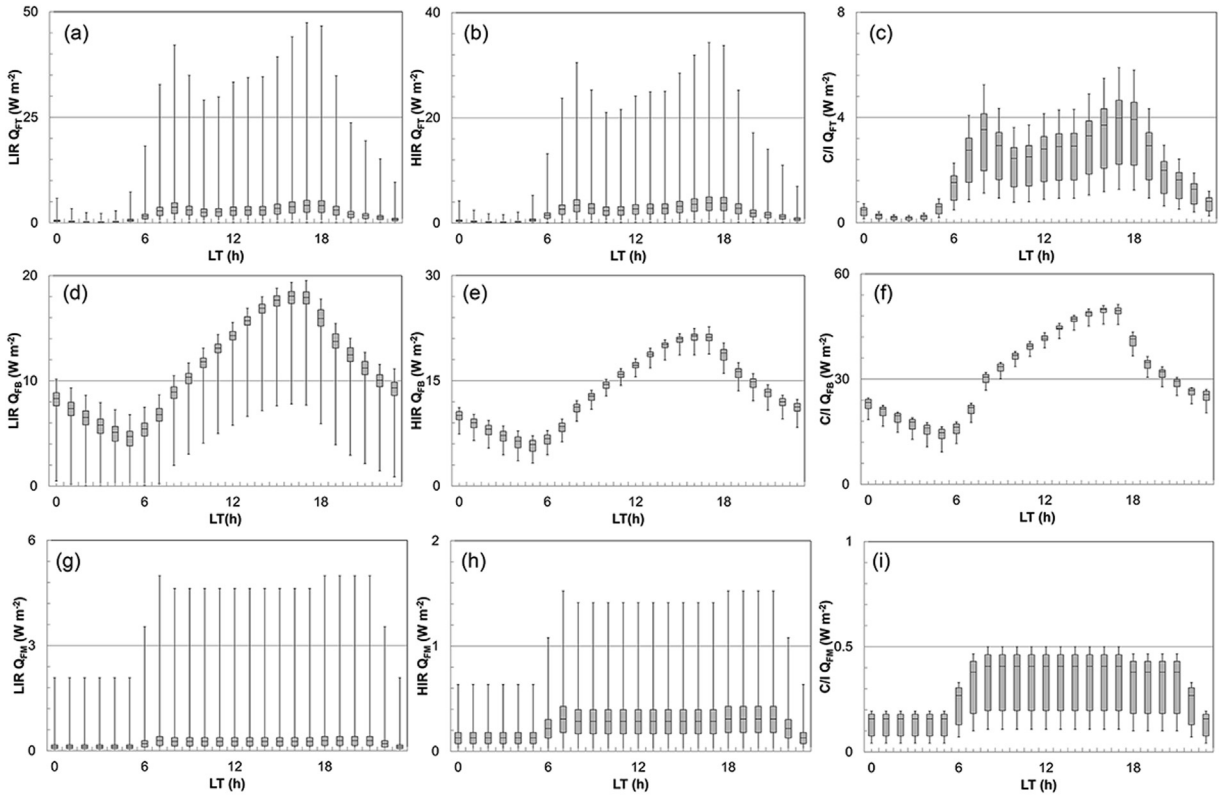

Fig. 12. Boxplots for each sub-component of multi-method Q_F ((a.–c.): Q_{FT}; (d.–f.): Q_{FB}, and (g.–i.): Q_{FM}), with data for LIR within the left column; HIR in the middle column, and C/I in the right column.

The spatial distribution of regional scale Q_F share similarities with UHI research that determined urban temperature fields in Phoenix through observations from weather stations (e.g. Brazel et al., 2007) or from physical climate modeling (e.g. Georgescu et al., 2012). This relationship is best observed with respect to how high magnitudes of Q_F within C/I areas correspond well to locations in which maximum urban temperatures are usually documented. The regional maps of average daily and maximum Q_F are similar to nighttime UHI maps in which highest temperatures are generally observed at the urban core. As the UHI is generally a nocturnal phenomenon best discerned in the early evening hours in Phoenix (e.g. Sun et al., 2009), analysis of hourly Q_F across different land covers in the period after sunset would yield additional insights into the contribution of waste heat towards UHI development. In other cities such as London (Bohnenstengel et al., 2013) and Singapore (Li et al., 2013), Q_F comparisons through inventory approaches with regional climate model simulations of near-surface temperature have noted periods where Q_F is potentially a major component of the urban surface energy balance and UHI development. While such comparisons of complete Q_F have not been done hitherto in Phoenix, a 10-day WRF simulation coupled to BEP + BEM examined the influence of just Q_{FB} during an extreme heat event indicating that nocturnal local-scale urban temperatures can be increased by 1 °C from the corresponding rise in electrical consumption due to AC use (Salamanca et al., 2014).

The additional input of Q_F at regional scales could also imply modifications in the urban boundary layer. Observed mean summer nocturnal Q_H fluxes are notably both low (<10 W m^{-2}) in magnitude and negative in sign (i.e. stable near-surface conditions that inhibit turbulence) in the immediate post–sunset period measured by EC at WPHX sited within a HIR area (Chow et al., 2014). Salamanca et al. (2014) illustrated that the additional release of Q_{FB} from just AC use modifies the thermal stratification of the urban boundary layer during the early evening by enhancing vertical mixing close to the surface. It is likely that with the additional inputs of Q_{FM} and Q_{FT}, especially in C/I areas where post–sunset Q_F are consistently >20 W m^{-2}, could augment mixing of the near-surface urban boundary layer. The increase in turbulence likely enhances urban warming, and suggests that Q_F could be a larger factor in nocturnal UHI causation at least for this study area. More research on the link between Q_F emissions to variations in local (e.g. within urban neighborhoods) and regional (e.g. for the entire metropolitan area) UHI intensities could be subsequently done to examine this possible relationship in Phoenix.

5. Conclusion

Using a framework proposed by Sailor (2011), anthropogenic heat emissions in a major metropolitan area – Phoenix, AZ – were estimated using a combination of inventory methods for traffic and human metabolism emissions, as well as through simulations of waste heat generated by electrical consumption of air conditioning use from a coupled Building Energy (BEM + BEP) – Regional Climate Model (WRF). Traffic emissions were estimated from publicly available traffic count data that were compiled for the entire metropolitan area, and human metabolism emissions were estimated from recent U.S. Census data. The combined Q_F were subsequently compiled and mapped through GIS for the summer months at various time scales (i.e. hourly, daily, and monthly). These local- and regional-scale estimates of Q_F were compiled during the summer months, and were compared to previous estimates of Q_F from the inventory method as well as through daily SEB residuals from an eddy covariance flux tower sited in a Phoenix residential area.

We found that despite the complexities and implicit errors from the inter-comparison and validation of Q_F between differing approaches for a local-scale residential area, there are reasonable similarities in flux densities between the multi-method Q_F applied in this study with both derived energy balance residuals and an inventory approach at least for the diurnal 24 h period. The multi-method approach also suggests that summer Q_F in Phoenix is sensitive to precipitation events, mostly arising through lower electrical use (i.e. reduced Q_{FB}), resulting in a decrease of ~2–5 W m^{-2}. At regional scales, we mapped and analyzed Q_F and discerned distinct spatial variations of both mean daily and maximum Q_F across different land uses, and highlighted the relative significance of traffic and urban electrical consumption – and the corresponding insignificance of human metabolism – towards the generation of Q_F. Results also suggest that the influence of Q_F inputs into the urban climate could be important towards the development of the Phoenix UHI in two ways. First, through notably higher magnitudes of estimated Q_F across most land cover classes vs. previous observed fluxes of Q_H from a residential EC flux tower, especially during the early evening in which large UHI intensities are usually documented. Second, through increasing turbulent vertical mixing and the size of the urban boundary layer, which potentially enhances the nocturnal UHI in Phoenix in terms of its horizontal and vertical extent.

We suggest that this multi-method approach is useful towards improving the potential accuracy and sensitivity of Q_F estimates for urban areas, particularly over multiple spatio-temporal scales. While caveats specific to the multi-method approach employed in this study have been previously stated, other considerations affecting its suitability in other areas should also be mentioned. Quality-controlled, up-to-date traffic, population and electrical consumption data needed for estimating Q_{FT}, Q_{FM} and Q_{FB} may not be readily available. Heating fuel data in residential or industrial areas may be needed depending on local climate and time of year, although these data are often difficult to obtain at the appropriate spatio-temporal scale. The absence of observed urban SEB data through either EC or scintillometery measurements would also prohibit the essential validation of this approach; this would appear to be a major limiting factor in applying this method, although there is a growing number of deployed urban SEB towers in which data could effectively be utilized (Grimmond and Christen, 2012). In conclusion, the influence of Q_F has been previously underrepresented in research compared to other aspects of urban climate, and much more work is required to gain a more comprehensive understanding of its effect on the near-surface atmosphere. This study thus complements other research that examines the influence of Q_F towards across different scales e.g. global (Allen et al., 2010), regional (Li et al., 2003) and local (Pigeon et al., 2007). These results can potentially aid in constraining future Q_F estimates when applied to local-scale (or finer resolution) urban climate modeling; for instance, spatially explicit Q_F inputs estimated from this method could minimize potential inaccuracies via the non-representation of waste heat inputs into the urban system, and allow for model applications towards assessing impacts through adaptation and mitigations policies that focus on reducing urban waste heat.

Acknowledgments

This research was funded by the National Science Foundation through DMS-1419593 (PI: AM), Earth Systems Models (EaSM) Program Award #1049251 (PI: BLR), and DEB-9714833 (Central Arizona-Phoenix Long Term Ecological Research III). The critical comments from the editor and reviewers of this study's initial draft are also much appreciated. Any opinions, findings, and conclusions or recommendation expressed in this material are those of the authors and do not necessarily reflect the views of the National Science Foundation. WTLC was also funded by the National University of Singapore Research Grant R-109-000-162-133.

References

Allen, L., Lindberg, F., Grimmond, C.S.B., 2010. Global to city scale urban anthropogenic heat flux; model and variability. Int. J. Climatol. 31, 1990–2005.
Arizona Department of Transportation, 2010. State Highway Traffic Log. Available from: https://www.azdot.gov/docs/planning/currentaadt.pdf?sfvrsn=4.
Aubinet, M., Vesala, T., Papale, D. (Eds.), 2012. Eddy Covariance: a Practical Guide to Measurement and Data Analysis. Springer, New York, NY.
Bohnenstengel, S.I., Hamilton, I., Davies, M., Belcher, S.E., 2013. Impact of anthropogenic heat emissions on London's temperatures. Q.J.R. Meteorol. Soc. 140 (679), 687–698.
Brazel, A.J., Gober, P., Lee, S.-J., Grossman-Clarke, S., Zehnder, J., Hedquist, B., Comparri, E., 2007. Determinants of changes in the regional urban heat island in metropolitan Phoenix (Arizona, USA) between 1990 and 2004. Clim. Res. 33, 171–182.
Burian, S.J., Velugubantla, S.P., Brown, M.J., 2002. Morphological Analyses Using 3D Building Databases: Phoenix, Arizona (LA-UR-02-6726). Los Alamos National Laboratory, pp. 1–65.
Chow, W.T.L., Brennan, D., Brazel, A.J., 2012. Urban heat island research in Phoenix, Arizona: theoretical contributions and policy applications. Bull. Am. Meteorol. Soc. 93 (4), 517–530.
Chow, W.T.L., Volo, T.J., Vivoni, E.R., Jenerette, G.D., Ruddell, B.L., 2014. Seasonal dynamics of a suburban energy balance in Phoenix, Arizona. Int. J. Climatol. http://dx.doi.org/10.1002/joc.3947.
Christen, A., Vogt, R., 2004. Energy and radiation balance of a central European city. Int. J. Climatol. 24, 1395–1421.
City of Phoenix, 2010. Traffic Volume Map. Available from: http://phoenix.gov/streets/traffic/volumemap.
Declet-Barreto, J., Brazel, A.J., Martin, C.A., Chow, W.T.L., Harlan, S.L., 2013. Creating the park cool island in an inner-city neighborhood: heat mitigation strategy for Phoenix, AZ. Urban Ecosyst. 16, 617–635.
Dhakal, S., Hanaki, K., 2002. Improvement of urban thermal environment by managing heat discharge sources and surface modification in Tokyo. Energy Build. 34 (1), 13–23.
Fan, H., Sailor, D.J., 2005. Modeling the impacts of anthropogenic heating on the urban climate of Philadelphia: a comparison of implementations in two PBL schemes. Atmos. Environ. 39 (1), 73–84.
Fanger, P.O., 1972. Thermal Comfort: Analysis and Applications in Environmental Engineering. McGraw-Hill, New York.
Fernando, H.J.S., Zajic, D., Di Sabatino, S., Dimitrova, R., Hedquist, B., Dallman, A., 2010. Flow, turbulence, and pollutant dispersion in urban atmospheres). Phys. Fluids 22 (5), 051301.
Foken, T., 2008. The energy balance closure problem: an overview. Ecol. Appl. 18 (6), 1351–1367.
Fry, J.A., Xian, G., Jin, S., Dewitz, J.A., Homer, C.G., Yang, L.M., Barnes, C.A., Herold, N.D., Wickham, J.D., 2011. Completion of the 2006 national land cover database for the conterminous United States. Photogramm. Eng. Remote Sens. 77 (9), 858–864.
Georgescu, M., Moustaoui, M., Mahalov, A., Dudhia, J., 2013. Summer-time climate impacts of projected megapolitan expansion in Arizona. Nat. Clim. Change 3, 37–41.
Georgescu, M., Mahalov, A., Moustaoui, M., 2012. Seasonal hydroclimatic impacts of Sun Corridor expansion. Environ. Res. Lett. 7 (3), 034026.
Gober, P., 2006. Metropolitan Phoenix: Place Making and Community Building in the Desert. University of Pennsylvania Press, Philadelphia.
Grimmond, C.S.B., 1992. The suburban energy balance: methodological considerations and results for a mid-latitude west coast city under winter and spring conditions. Int. J. Climatol. 12, 481–497.
Grimmond, C.S.B., Christen, A., 2012. Flux measurements in urban ecosystems. Fluxnet Newsl. 5 (1), 1–8.
Grimmond, C.S.B., Roth, M., Oke, T.R., Au, Y.C., Best, M., Betts, R., Carmichael, G., Cleugh, H., Dabberdt, W., Emmanuel, R., Freitas, E., Fortuniak, K., Hanna, S., Klein, P., Kalkstein, L.S., Liu, C.H., Nickson, A., Pearlmutter, D., Sailor, D.J., Voogt, J., 2010. Climate and more sustainable cities: climate information for improved planning and management of cities (producers/capabilities perspective). Procedia Environ. Sci. 1, 247–274.
Grossman-Clarke, S., Zehnder, J.A., Stefanov, W.L., Liu, Y., Zoldak, M.A., 2005. Urban modifications in a mesoscale meteorological model and the effects on near-surface variables in an arid metropolitan region. J. Appl. Meteorol. 44, 1281–1297.
Hallenbeck, M., Rice, M., Smith, B., Cornell-Martinez, C., Wilkinson, J., 1997. Vehicle Volume Distribution by Classification. Washington State Transportation Center, p. 54. University of Washington, 1107 NE 45th St. Suite 535, Seattle WA 98105. http://depts.washington.edu/trac.

Harlan, S.L., Brazel, A.J., Prashad, L., Stefanov, W.L., Larsen, L., 2006. Neighborhood microclimates and vulnerability to heat stress. Soc. Sci. Med. 63, 2847–2863.
Hill, R.W., Muhich, T.E., Humphries, M.M., 2013. City-scale expansion of human thermoregulatory costs. PLOS One 8 (10), e76238.
Hondula, D.M., Georgescu, M., Balling Jr., R.C., 2014. Challenges associated with projecting urbanization-induced heat-related mortality. Sci. Total Environ. 490, 538–544.
Iamarino, M., Beevers, S., Grimmond, C.S.B., 2012. High-resolution (space, time) anthropogenic heat emissions: London 1970–2025. Int. J. Climatol. 32 (11), 1754–1767.
Ichinose, T., Shimodozono, K., Hanaki, K., 1999. Impact of anthropogenic heat on urban climate in Tokyo. Atmos. Environ. 33, 3897–3909.
Kim, C., Park, Y.-S., Sang, S., 2008. Spatial and temporal analysis of urban traffic volume. In: Proceedings from the 2008 ESRI International User Conference, p. 24. Available from: http://proceedings.esri.com/library/userconf/proc08/papers/papers/pap_1613.pdf.
Lee, S.M., Fernando, H.J., Princevac, M., Zajic, D., Sinesi, M., McCulley, J.L., Anderson, J., 2003. Transport and diffusion of ozone in the nocturnal and morning planetary boundary layer of the Phoenix valley. Environ. Fluid Mech. 3 (4), 331–362.
Lee, S.H., Song, C.K., Baik, J.J., Park, S.U., 2009. Estimation of anthropogenic heat emission in the Gyeong-In region of Korea. Theor. Appl. Climatol. 96 (3–4), 291–303.
Li, X.X., Koh, T.Y., Entekhabi, D., Roth, M., Panda, J., Norford, L.K., 2013. A multi-resolution ensemble study of a tropical urban environment and its interactions with the background regional atmosphere. J. Geophys. Res. Atmos. 118 (17), 9804–9818.
Lindberg, F., Grimmond, C.S.B., Yogeswaran, N., Kotthaus, S., Allen, L., 2013. Impact of city changes and weather on anthropogenic heat flux in Europe 1995–2015. Urban Clim. 4, 1–15.
Magee, N., Curtis, J., Wendler, G., 1999. The urban heat island effect at Fairbanks, Alaska. Theor. Appl. Climatol. 64 (1–2), 39–47.
Maricopa Association of Governments, 2011. 2011 Average Weekday Traffic Volume Map. Available from: http://www.azmag.gov/Documents/TRANS_2013-10-08_2011-Average-Weekday-Traffic-Volume-Map.pdf.
Maricopa County Department of Transportation, 2012. Maps and Technical Documents: Traffic Counts. Available from: http://www.mcdot.maricopa.gov/technical/counts/home.htm.
Martilli, A., Clappier, A., Rotach, M.W., 2002. An urban surface exchange parameterization for mesoscale models. Boundary-Layer Meteorol. 104 (2), 261–304.
Offerle, B., Grimmond, C.S.B., Fortuniak, K., 2005. Heat storage and anthropogenic heat flux in relation to the energy balance of a central European city centre. Int. J. Climatol. 25, 1405–1419.
Oke, T.R., 1982. The energetic basis of the urban heat island. Q. J. R. Meteorological Soc. 108, 1–24.
Oke, T.R., 1988. The urban energy balance. Prog. Phys. Geogr. 12, 471–508.
Oke, T.R., 2006. Towards better scientific communication in urban climate. Theor. Appl. Climatol. 84, 179–190.
Oke, T.R., Zeuner, G., Jauregui, E., 1992. The surface energy balance in Mexico City. Atmos. Environ. 26B, 433–444.
Pigeon, G., Legain, D., Durand, P., Masson, V., 2007. Anthropogenic heat release in an old European agglomeration (Toulouse, France). Int. J. Climatol. 27, 1969–1981.
Quah, A.K.L., Roth, M., 2012. Diurnal and weekly variation of anthropogenic heat emissions in a tropical city, Singapore. Atmos. Environ. 46, 92–103.
Sailor, D.J., 2011. A review of methods for estimating anthropogenic heat and moisture emissions in the urban environment. Int. J. Climatol. 31, 189–199.
Sailor, D.J., Lu, L., 2004. A top-down methodology for developing diurnal and seasonal anthropogenic heating profiles for urban areas. Atmos. Environ. 38 (17), 2737–2748.
Salamanca, F., Martilli, A., 2010. A new building energy model coupled with an urban canopy parameterization for urban climate simulations – part II. Validation with one dimension off-line simulations. Theor. Appl. Climatol. 99 (3–4), 345–356.
Salamanca, F., Krpo, A., Martilli, A., Clappier, A., 2010. A new building energy model coupled with an urban canopy parameterization for urban climate simulations – part I. formulation, verification, and sensitivity analysis of the model. Theor. Appl. Climatol. 99 (3–4), 331–344.
Salamanca, F., Georgescu, M., Mahalov, A., Moustaoui, M., Wang, M., Svoma, B.M., 2013. Assessing summertime urban air conditioning consumption in a semiarid environment. Environ. Res. Lett. 8 (3), 034022.
Salamanca, F., Georgescu, M., Mahalov, A., Moustaoui, M., Wang, M., 2014. Anthropogenic heating of the urban environment due to air conditioning. J. Geophys. Res. Atmos. 119 http://dx.doi.org/10.1002/2013JD021225.
Simmonds, I., Keay, K., 1997. Weekly cycle of meteorological variations in Melbourne and the role of pollution and anthropogenic heat release. Atmos. Environ. 31 (11), 1589–1603.
Skamarock, W.C., Klemp, J.B., Dudhia, J., Gill, D.O., Barker, D.M., Duda, M.G., Huang, X.-Y., Wang, W., Powers, J.G., 2008. A Description of the Advanced Research WRF Version 3. NCAR Tech. Note NCAR/TN-475+STR. National Center for Atmospheric Research, Boulder, CO, p. 125.
Stefanov, W.L., Ramsey, M.S., Christensen, P.R., 2001. Monitoring urban land cover change: an expert system approach to land cover classification of semiarid to arid urban centers. Remote Sens. Environ. 77, 173–186.
Sun, C.Y., Brazel, A.J., Chow, W.T.L., Hedquist, B.C., Prashad, L., 2009. Desert heat island study in winter by mobile transect and remote sensing techniques. Theor. Appl. Climatol. 98 (3–4), 323–335.
Taha, H., 1997. Urban climates and heat islands: albedo, evapotranspiration, and anthropogenic heat. Energy Build. 25, 99–103.
United States Census Bureau, 2000. Commuter-adjusted Daytime Population 2000. Available at: http://www.census.gov/hhes/commuting/data/census2000.html.
United States Census Bureau, 2010. Demographic Profiles: Arizona. Available at: http://www.census.gov/2010census/news/press-kits/demographic-profiles.html.
United States Department of Transportation, 2011. Annual Vehicle Distance Travelled in Miles and Related Data – 2010 (1.) by Highway Category and Vehicle Type. Available from: http://www.fhwa.dot.gov/policyinformation/statistics/2010/pdf/vm1.pdf.
United States Energy Information Administration, 2014. Petroleum & Other Liquids: Gasoline and Diesel Fuel Update. Available from: http://www.eia.gov/petroleum/gasdiesel/diesel_proc-methods.cfm.
U.S. Federal Highway Administration, 2013. Office of Highway Policy Information: Travel Monitoring – Traffic Volume Trends. Available from: http://www.fhwa.dot.gov/policyinformation/travel_monitoring/tvt.cfm.
Ward, H.C., Evans, J.G., Grimmond, C.S.B., 2013. Multi-season eddy covariance observations of energy, water and carbon fluxes over a suburban area in Swindon, UK. Atmos. Chem. Phys. 13, 4645–4666.
Willmott, C.J., 1982. Some comments on the evaluation of model performance. Bull. Am. Meteorological Soc. 63 (11), 1309–1313.
Wolman, A., 1965. The metabolism of cities. Sci. Am. 213 (3), 179–190.
Zhang, G.J., Cai, M., Hu, A., 2013. Energy consumption and the unexplained winter warming over northern Asia and North America. Nat. Clim. Change 3, 466–470.